A Pipeline for Computer Aided Polyp Detection

Wei Hong, Feng Qiu, and Arie Kaufman, *Fellow, IEEE*

Abstract—We present a novel pipeline for computer-aided detection (CAD) of colonic polyps by integrating texture and shape analysis with volume rendering and conformal colon flattening. Using our automatic method, the 3D polyp detection problem is converted into a 2D pattern recognition problem. The colon surface is first segmented and extracted from the CT data set of the patient's abdomen, which is then mapped to a 2D rectangle using conformal mapping. This flattened image is rendered using a direct volume rendering technique with a translucent electronic biopsy transfer function. The polyps are detected by a 2D clustering method on the flattened image. The false positives are further reduced by analyzing the volumetric shape and texture features. Compared with shape based methods, our method is much more efficient without the need of computing curvature and other shape parameters for the whole colon surface. The final detection results are stored in the 2D image, which can be easily incorporated into a virtual colonoscopy (VC) system to highlight the polyp locations. The extracted colon surface mesh can be used to accelerate the volumetric ray casting algorithm used to generate the VC endoscopic view. The proposed automatic CAD pipeline is incorporated into an interactive VC system, with a goal of helping radiologists detect polyps faster and with higher accuracy.

Index Terms—Computer Aided Detection, Virtual Colonoscopy, Texture Analysis, Volume Rendering

1 Introduction

Colorectal cancer is the second leading cause of cancer-related deaths in the United States. Most colorectal cancers are believed to arise within benign adenomatous polyps that develop slowly over the course of many years [18]. Evidence-based guidelines recommend the screening of adults who are at average risk for colorectal cancer, since the detection and removal of adenomas has been shown to substantially reduce the incidence of cancer and cancer-related mortality. Therefore, many have advocated screening programs to detect polyps with a diameter of less than one centimeter [14]. However, most people do not follow this advice because of the discomfort and inconvenience of the traditional optical colonoscopy (OC).

To encourage people to participate in screening programs, *virtual colonoscopy (VC)*, also known as *computed tomographic colonography (CTC)*, has been proposed and developed to detect colorectal neoplasms by using a computed tomography (CT) scan [9, 11]. A single breath-hold scan of the patient's abdomen usually generates 400-700 512×512 CT axial images. VC is minimally invasive, fast, inexpensive, and examines 100% of the colon wall. It does not require sedation nor the insertion of a colonoscope, and uses only a minimal bowel preparation of a modified diet with oral contrast agent (e.g., barium) for tagging residual stool and luminal fluid. VC exploits computers to reconstruct a 3D colon model from the CT scan, and create a virtual model of the whole colon to help radiologists navigate the model for diagnosis. Pickhardt et al. [18] have demonstrated that the performance of a VC compares favorably with that of a traditional OC. Because of the complex structure of the colon surface, the inspection is prone to errors, and the radiologist needs to navigate antegrade (from rectum to cecum) and retrograde (from cecum to rectum) to improve the coverage and accuracy of the inspection. A complete inspection by a radiologist conducting 3D VC takes 10-15 minutes [11].

The long interpretation effort of the VC screening procedure suggests a *computer-aided detection (CAD)* approach. A CAD scheme that automatically detects the locations of the potential polyp candidates could substantially reduce the radiologists' interpretation time and improve their diagnostic performance with higher accuracy. However, the automatic detection of colonic polyps is a very challenging task because polyps can occur in various sizes and shapes. Moreover, there are numerous colon folds and residual colonic materials on the colon wall that mimic polyps and could result in false positives (FPs). A CAD scheme should have the ability to identify true polyps and eliminate the FPs.

The main contributions of this paper are: (1) using direct volume rendering to generate electronic biopsy images for polyp detection, (2) devising a voxel based topological denoising algorithm to remove tiny handles in the volume, (3) introducing a novel pipeline for polyp detection, (4) converting the polyp detection problem from 3D to 2D using conformal colon flattening, (5) providing a flattened colon view in the user interface to enhance the VC system, and (6) highlighting the suspicious polyp candidates in the endoscopic view to guarantee that no polyp is missed in our VC system.

The remainder of this paper is organized as follows. We first briefly discuss the related work in Section 2. Our CAD pipeline is presented in Section 3. Section 4 describes the integration of polyp detection results with VC. The implementation and experimental results are reported in Section 5. In Section 6, concluding remarks are drawn and future work is summarized.

2 Related Work

In the past several years there have been several prototype CAD schemes reported in the literature with variable success of polyp detection. Shape and texture features are the two major characteristic features that have been used to differentiate polyps from normal soft tissues. Vining et al. [21] have utilized the measure of abnormal colon wall thickness to detect polyp suspects. Summers et al. [19] have employed local variations in curvature of the surface of the colonic wall to detect abnormal shapes. Then, the candidates are filtered by the restrictions of mean curvature, dimensionless ratio sphericity, and minimum polyp size to reduce FPs. Although our method also extracts the surface of the colonic wall, it is used only for mapping the features from 3D to 2D. The features used for polyp detection in our method are still computed in the 3D volume. Paik et al. [17] have observed that normals on the colon surface usually intersect with normals on neighboring surfaces, as polyps have 3D shape features changing rapidly in many directions. Based on this observation, they have introduced a method to detect polyps by the number of intersecting normal vectors of a patch. Yoshida et al. [28] and Nappi et al. [15] have further characterized the curvature measures by shape index and curvedness to differentiate polyps from colonic folds and the colon wall. The volumetric features gradient concentration (GC) and directional gradient concentration (DGC) are used for reducing FPs. Based on the assumption that polyps are composed of small, approximately spherical patches, Tomasi and Göktürk [20] have designed a method of lo-

• *W. Hong, F. Qiu, and A. Kaufman are with the Department of Computer Science, Stony Brook University, Stony Brook, NY 11794-4400. Email: weihong, qfeng, ari@cs.sunysb.edu.*

Manuscript received 31 March 2006; accepted 1 August 2006; posted online 6 November 2006.
For information on obtaining reprints of this article, please send e-mail to: tvcg@computer.org.

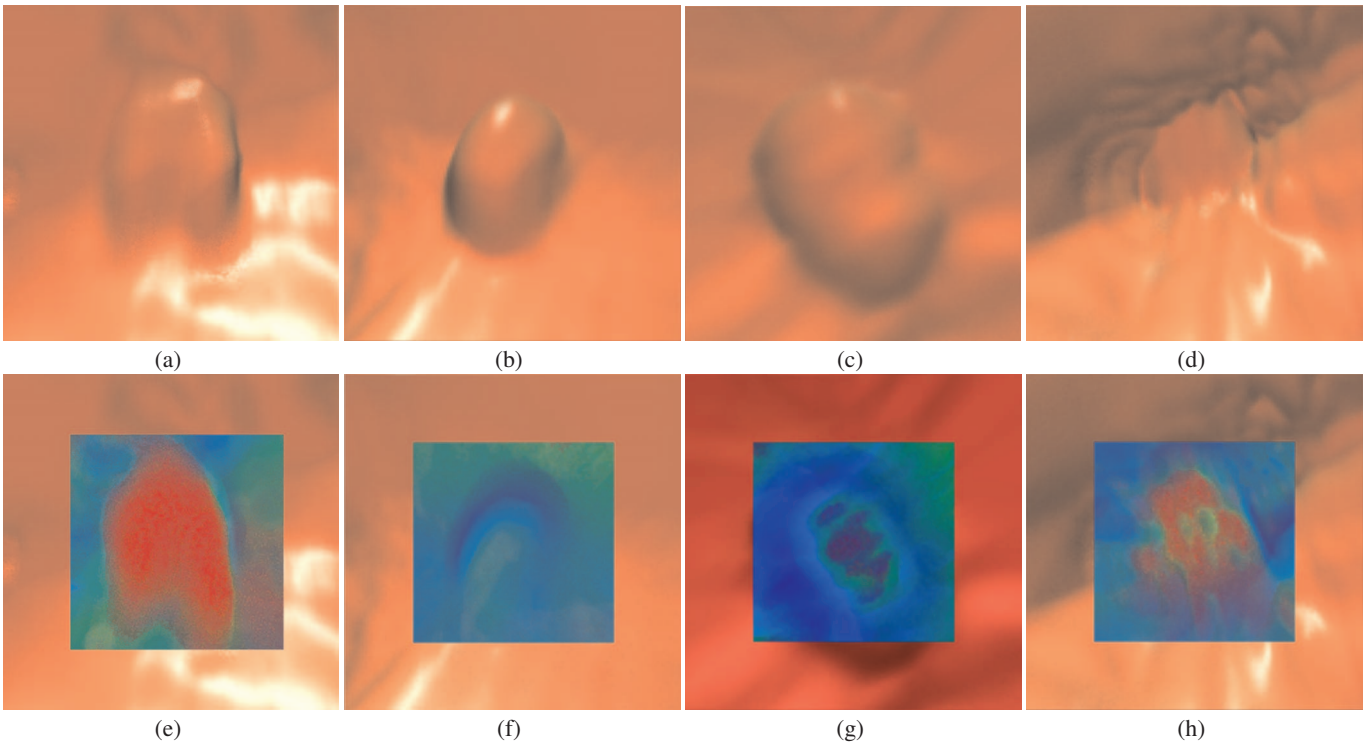

Fig. 1. (a)-(d) are the surface rendering of (a) retained stool, (b) a hyperplastic polyp, (c) an adenoma, and (d) a tubulovillous adenoma. The small square images in (e)-(h) are the electronic biopsy rendering of the respective objects in (a)-(d), all with same transfer function. In the electronic biopsy images, the red color represents the highest densities and blue represents the lowest densities. Green represents tissues of middle densities. Normal tissues have low to middle densities.

cally fitting a sphere to the isosurface of each voxel on the colon wall. Groups of voxels having many neighboring spheres are considered as polyp candidates. Kiss et al. [12] have utilized normal and sphere fitting as the references to extract some geometric features on the polyp surfaces. Wang et al. [24] have introduced a new shape description global curvature for polyp detection. All these shape based methods are sensitive to the irregularity of the colon wall and therefore share a relatively high FP rate, which is undesirable.

Göktürk et al. [6] have presented a statistical approach that uses support vector machines to distinguish the differentiating characteristics of polyps and healthy tissue, and use this information for the classification of the new cases. Acar et al. [1] have proposed a CAD scheme using an edge-displacement field to analyze and improve the polyp detection. Nappi et al. [16] employed a conditional morphological dilation strategy to extract the suspected regions. The FPs are reduced by further analyzing three shape features from these suspicious regions. Yao et al. [26] have explored image segmentation methods in CAD to reduce the FPs. This method is based on a combination of knowledge-guided intensity adjustment, fuzzy c-mean clustering, and deformable models. The volumetric features computed from the segmentation can further reduce FPs.

In our earlier work [22], we have observed that the internal tissues of polyps have a slightly higher density and different texture than healthy tissues. These high density areas are beneath the colon wall and cannot be seen with an optical colonoscopy. However, the internal structure of polyps can be revealed through volume rendering with a translucent transfer function, called *electronic biopsy*. The four images of Figures 1(e)-(h) are the electronic biopsy images of the four corresponding objects of Figures 1(a)-(d). Although polyps and normal tissues may have similar shapes, it is observed that adenomatous and malignant polyps have a higher density and different texture beneath the surface. As shown in Figure 1, four different objects including retained stool, a hyperplastic polyp, an adenoma, and a tubulovillous adenoma have different rendering results for the same transfer function. The retained stool has a uniform high density inside the whole object with sharp boundaries due to the oral agent tagging. The hyperplastic polyp is benign and does not have any high density voxels. The adenoma and tubulovillous adenoma are neoplastic with irregular internal structures and high density voxels gradually change to normal tissues towards the boundary. These observations suggest that polyps can be detected by analyzing the electronic biopsy images of the whole colon.

In our method, we conformally map the colon surface to a 2D rectangle, which simplifies the polyp detection problem from 3D to 2D. Our polyp detection method is then applied on high-quality 2D electronic biopsy images generated with a volumetric ray-casting algorithm. Unlike previous shape based methods, in which shape information is computed for polyp detection in the entire colon, we only compute the shape information at suspicious regions in order to reduce FPs.

3 Our Pipeline

A diagram of our CAD pipeline is shown in Figure 2. First, for segmentation and digital cleansing of the colon, an iterative partial volume segmentation algorithm is applied. Then, a topologically simple colon surface is extracted for conformal colon flattening. The electronic biopsy colon image is then generated using a volumetric ray casting algorithm on the entire flattened colon. After that, our clustering algorithm and reduction of FPs are performed. All of these processes are performed automatically in our pipeline. The details of each step are discussed in the following subsections.

3.1 Segmentation and Digital Cleansing

This step aims to segment the colon lumen from the patient's abdominal data set acquired using CT and an oral contrast agent for colonic material tagging, and to cleanse the colon lumen of all tagged material, so that a cleansed virtual colon model can be constructed. In general, there exist two major challenges for digital cleansing. The first is the removal of the interface layer between the air and the tagged colonic

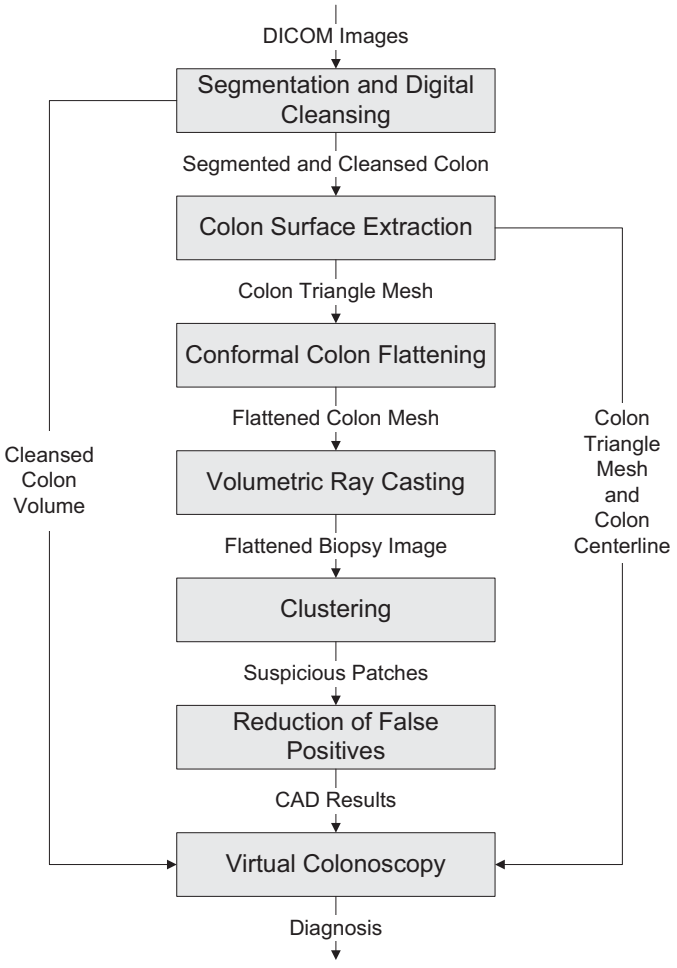

Fig. 2. Overview of our CAD pipeline.

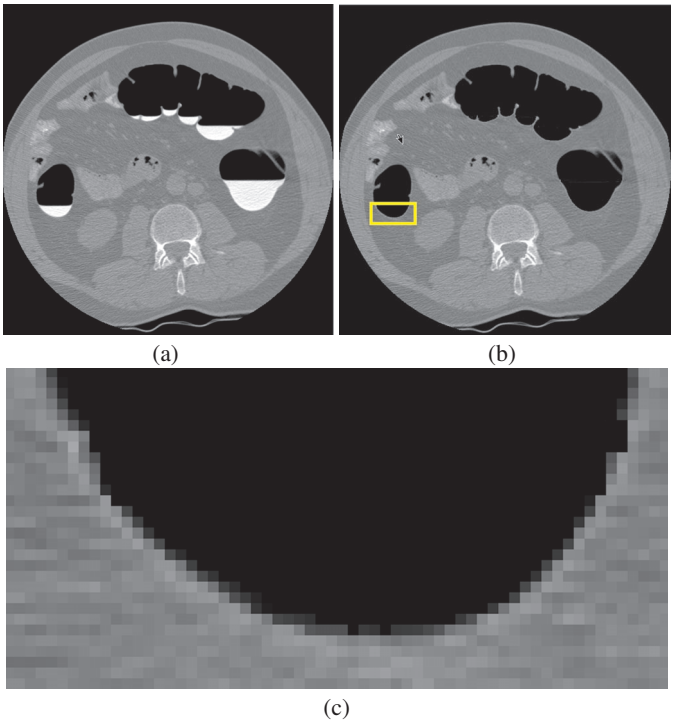

Fig. 3. The result of digital cleansing. (a) An original CT image (slice), (b) the corresponding cleansed slice, and (c) a zoomed-in view of the cleansed region in (b).

materials. Due to the partial volume effect, this layer covers the density values of colon tissues and so it is impossible to distinguish the voxels of colonic materials in this layer from that of the colon tissues. Another challenge is the restoration of the CT density values of colon tissues in the enhanced mucosa layer and the removal of the portion with tagged colonic materials. Partial volume image segmentation [25] is a desirable approach to identify the layers, quantify the material/tissue mixtures in the layers and restore the true CT density values of the colon mucosa layer.

We first applied an iterative partial volume segmentation algorithm [25]. The voxels in the colon lumen are classified as air, mixture of air with tissue, mixture of air with tagged materials, or mixture of tissue with tagged materials. Then, the interface layer is identified by the dilation and erosion method. The equation used to restore the CT density values of the colon tissues in the enhanced mucosa layer can be found in [25]. After this step, we obtain a segmentation of the colon and a clean colon lumen. One original CT axial image (slice) and the corresponding cleansed slice are shown in Figures 3(a) and 3(b), respectively. A zoomed-in view of the region bounded by the yellow box in Figure 3(b) is shown in Figure 3(c).

3.2 Colon Surface Extraction

After segmentation and digital cleansing, we need to extract the colon surface for our conformal virtual colon flattening algorithm. The topological noise makes our flattening algorithm complex and introduces distortion. We previously used a shortest loop method [10] to detect and cut handles to remove the topological noise after extracting the colon surface. Han et al. [8] have presented a topology preserving level set method, which achieves topology preservation by applying the simple point concept from digital topology [4]. They conclude that it is only necessary to be concerned with topological changes when the level set function is changing sign. Therefore, in their method the level set function sign changes are only allowed at a simple point. In this method, a cut is obtained at each handle of the digital object to preserve topology. However, this method cannot guarantee that the cut of the handle is minimized. Moreover, solving the partial differential equations in the level set method results in a significant computational burden, especially when it is applied to volumetric data.

In this paper, we present a new volume based topological denoising algorithm to remove tiny handles (i.e., topological noise) from the segmented colon. Because we already have a segmentation of the colon, we incorporate the simple point concept in a region growing based algorithm to extract a topologically simple segmentation of the colon lumen. A point is *simple* if its addition to and removal from a digital object does not change the object topology. In other words, a point is simple if it is adjacent to just one object component and one background component. We show a 2D example with (4, 8) connectivity in Figure 4, in which the red point is a simple point and the yellow point is a non-simple point. To avoid the connectivity paradox, (6, 18), (18, 6), (6, 26) and (26, 6) are four pairs of compatible connectivity used in 3D digital topology. In order to guarantee that the extracted colon surface using our topology preserving dual contouring algorithm [29] is a manifold, 6-connectivity is used for the colon lumen and 18-connectivity is used for the background. Thus, we use the topological numbers [4] corresponding to the compatible connectivity pair (6, 18) to determine whether a voxel is simple. The topological number is equal to the number of connected components within its geodesic neighborhood. Therefore, if both of them are equal to one, the voxel is simple. The following definitions are from [4].

Definition 3.1 *Let $X \subset Z^3$ and $x \in Z^3$. The topological numbers relative to the point x and set X are:*
$T_6(x,X) = \#C_6[N_6^2(x,X)]$ *and*
$T_{18}(x,X) = \#C_{18}[N_{18}^2(x,X)]$,
where $C_n(X)$ stands for the set of all n-connected components of X,

$\#C_n(X)$ stands for the cardinal of $C_n(X)$, N_n^k is the geodesic neighborhood of x inside X of order k and it is defined recursively by:
$N_n^1(x,X) = N_n^*(x) \cap X$ and
$N_n^k(x,X) = \cup N_n(y) \cap N_{26}^*(x) \cap X, y \in N_n^{k-1}(x,X)$,
where $N_n^*(x)$ is n-neighborhood of x.

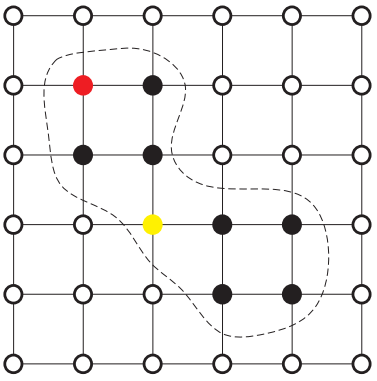

Fig. 4. Illustration of a simple point: the red point is a simple point, while the yellow point is not a simple point.

In our region growing algorithm, only the simple point is removed from the priority queue and marked as colon. Because a non-simple point may become simple when some points are added to the object, we decrease its priority by a small value δ ($\delta = 0.1$ in our current implementation) and insert it into the priority queue again if its priority is larger than a predefined threshold T_{th} ($T_{th} = 0.8$ in our current implementation). In order to guarantee that each handle is minimally cut, we use the distance from the boundary as a weight to control the region growing algorithm. The voxel with a larger distance from the colon wall has higher priority in our region growing algorithm. This can be implemented efficiently using a priority queue. Thus, we first compute an unsigned exact distance field using the segmented colon data obtained from the previous step. After that, we compute the skeleton (i.e., centerline) of the colon using the unsigned distance field, which is then used as the initial seeds set for region growing. Our topology preserving region growing algorithm is described as follows:

1. Mark the voxels of the input skeleton as colon.
2. For each voxel of the skeleton, put its six neighboring voxels into a priority queue Q.
3. While Q is not empty do
   (a) Let v be the top voxel in Q.
   (b) If v is a simple point, mark v as colon and put its six neighboring voxels into Q.
   (c) The priority of v is decreased by δ.
   (d) If the priority of v is greater than T_{th}, it is inserted into Q again.

After applying this algorithm, non-simple points are removed from the segmented colon. Thus, all tiny handles are removed. Then, we use our enhanced dual contour method [29] to extract a simplified smooth colon surface while preserving the topology of the finest resolution colon surface. A close up view of the colon surface extracted without our topological denoising algorithm is shown in Figure 5(a). Figure 5(b) shows the surface with topological denoising, and we can see that the two tiny handles on the right side are removed by our topological denoising algorithm. After this step, we obtain both the colon surface mesh with genus zero and the colon centerline.

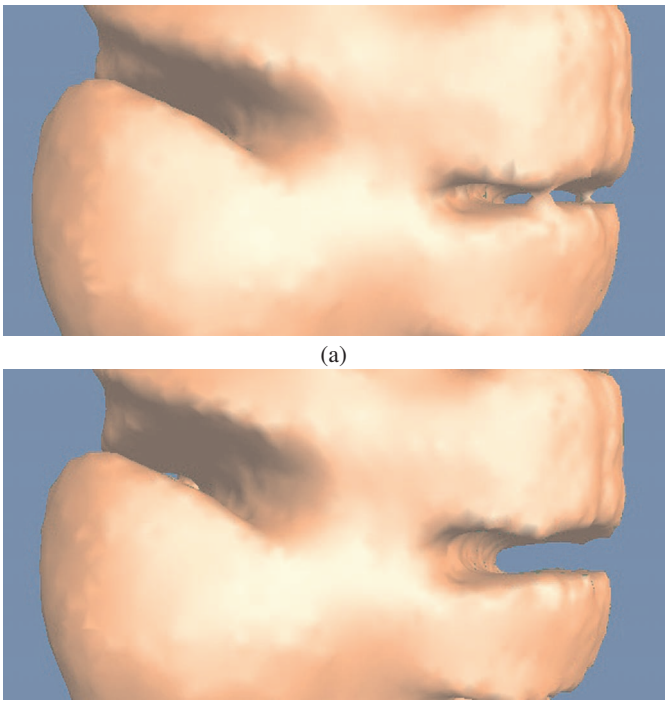

(a) (b)

Fig. 5. (a) A close up view of the colon surface extracted without topological denoising, and (b) a view of the colon surface extracted with topological denoising.

3.3 Conformal Virtual Colon Flattening

Virtual dissection is an efficient visualization technique for polyp detection, in which the entire inner surface of the colon is displayed as a single 2D image. The straightforward method [23] starts with uniformly resampling the colonic central path. At each sampling point, a cross section orthogonal to the path is computed. The central path is straightened and the cross sections are unfolded and remapped into a new 3D volume. The isosurface is then extracted and rendered for polyp detection. However, this method results in severe distortions. Several methods have been developed that are either area preserving [3] or angle preserving [7, 10].

We are specifically interested in an angle preserving method, because radiologists identify polyps mainly based on the shape information, and the lost area and volume information can be reconstructed by referring back to the original volumetric data. Haker et al.'s method [7] can only handle genus 0 surfaces, while our method [10] is more general and can handle high genus surfaces. In their method, the colon surface is mapped to a parallelogram, while in our method the colon surface is mapped to a rectangle. Moreover, they use coded mean curvature to color the colon surface. We instead use a volumetric ray-casting algorithm to generate a feature image for polyp detection. Since their method is based on the shape information computed from the colon surface, it requires a highly accurate and smooth surface mesh to achieve good mean curvature estimation. Moreover, they only discuss the flattening and rendering algorithm and not any computer-aided polyp detection algorithm.

In order to compute the conformal map between the colon surface and a 2D rectangle, we compute its gradient field first. Mathematically, this gradient field is called holomorphic 1-form. Then, the conformal mapping can be obtained by integration. Each gradient field of a conformal map is a pair of tangential vector fields with special properties, such as the curl and laplace are zero everywhere. All such vector fields form a linear space. We construct a basis of this linear space by solving a linear system derived from these properties. The global distortion from the colon surface to the parametric rectangle is minimized, which is measured by harmonic energy. The details of our

flattening algorithm can be found in [10].

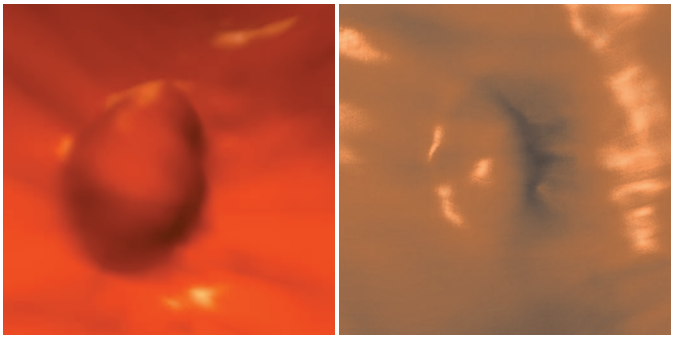

(a) (b)

Fig. 6. (a) A close up view of a polyp in an endoscopic view, (b) A view generated from the flattened colon image showing the same polyp.

As postulated in previous CAD papers, the colonic polyps usually have an elliptic curvature of the peak subtype, i.e., the shape at the top section of a regular polyp (toward the colon wall) is more likely to be a spherical cap. Because of the angle preservation of our colon flattening algorithm, the elliptic shape of a colonic polyp, as shown in Figure 6(a), is preserved in the flattened image, as shown in Figure 6(b). It is noted that our conformal colon flattening has area distortion. Consequently, polyps cannot be directly measured on the 2D flattened colon image. Since we maintain a one-to-one mapping between the 3D vertices and 2D vertices of the colon mesh, polyps can still be measured in 3D. Geometric features and texture features can also be computed in 3D and mapped to 2D. This conformal mapping simplifies our polyp detection problem from 3D to 2D. In the following section, we describe how to generate a 2D electronic biopsy image of the flattened colon.

3.4 2D Electronic Biopsy Image Generation

The electronic biopsy technique uses a volume rendering algorithm to present the information inside the colon wall on a 2D image, the biopsy image. Each voxel is assigned a specific color and opaque values according to its CT intensity. Then, the 3D volume is volume rendered and transformed into a 2D texture image based on our conformal mapping. This 2D texture image provides the intensity distribution information along each ray, which is hidden behind the colon surface.

In the canonical volumetric ray casting algorithm, a ray is shot for each pixel on the image plane. The direction of the ray is defined by the locations of the viewpoint and the pixel. When the ray hits the boundary of the volume, the ray starts to accumulate color and opacity values while stepping inside the volume. In our pipeline, a constrained volumetric ray casting algorithm is used to generate the 2D biopsy image. Each vertex of the mesh of the flattened colon has a 3D coordinate in the volume space. The coordinate of the first intersection point of each pixel is linearly interpolated from the three vertices of the triangle with which the ray intersects. Because flattening the colon into a 2D mesh is a nonlinear transformation, no one point can be defined as the viewpoint in the volume space for all rays. Therefore, we define the gradient at the intersection point as the direction of the ray. In our volumetric ray-casting algorithm, the sampling distance is 0.5mm. Because we are only interested in a thin layer (20mm) beneath the colon surface, each ray is only allowed to traverse up to 40 steps. Moreover, because the colon wall protrudes into the lumen, some rays may enter the colon lumen again. In order to avoid rays re-entering the colon lumen, these rays are terminated in our ray-casting algorithm using the segmentation information of the colon lumen. We can efficiently generate high resolution biopsy images accelerated on the GPU, where the thin layer beneath the colon wall is super-sampled. An electronic biopsy image is shown in Figure 9(a).

3.5 Clustering

It is observed that similar color features appear in contiguous areas in several regions of the 2D electronic biopsy image. It is reasonable to classify these features within a certain range in the 2D image. The RGB values of the given pixel and its twelve neighboring pixels form a 39-dimensional local feature vector. Consequently, a high resolution flattened electronic biopsy image is used in our CAD system, where each pixel has a 39-dimensional local feature vector. It requires intensive computational effort to manipulate such a large quantity of vectors. To reduce the computational burden, a feature analysis of the local vector series is necessary. The principal component analysis (PCA) is applied to the local vector series to determine the dimension of the feature vectors and the associated orthogonal transformation matrix (i.e., the K-L transformation matrix). The PCA on the training data sets shows that a reasonable dimension of the feature vectors is 7, where the summation of the first 7 principal components variances is more than 96.5% of the total variance.

The K-L transformation matrix is applied to the local vector series belonging to hand segmented polyps on the 2D flattened electronic biopsy images. In the K-L domain, the feature vectors are formed by the first 7 principal components from the transformed vector series. The mean vector of these feature vectors is computed and used as the representative vector V of the feature vectors belonging to polyps. The square root of the variance of these feature vectors is also computed and used as a threshold T for vector similarity in the clustering.

For a given testing data set, we use the representative vector V and similarity threshold T to classify the feature vectors in the K-L domain. If the Euclidean distance between a feature vector and V is less than T, the corresponding pixel is classified as belonging to a polyp. A 2D image is generated where the pixels classified belonging to a polyp are colored in red. The red regions in this 2D image are highly suspicious for being polyps, indicating that the physicians should observe these areas in the 3D view very carefully.

After the clustering algorithm, the pixels classified belonging to a polyp are marked. We first use a labeling algorithm to extract the connected components on this image. Since we only consider the polyps with a diameter larger than 5 mm, a component whose pixel count is below such a threshold is classified as a false-positive finding. Consequently, many small components are removed.

3.6 Reduction of False Positives

The false-positive findings can be further reduced by analyzing the shape features, such as the shape index and curvedness [28], as well as volumetric texture features [27]. The shape index is a measure of the shape. Every distinct shape, except for the plane, corresponds to a unique value of the shape index. The shape index values increase smoothly from the top section to the bottom peripheral region of a polyp on the colon wall inner surface. The curvedness represents how gently curved the surface is. Curvedness is a dual feature to the shape index in that the shape index measures which shape the local neighborhood of a voxel has, whereas the curvedness measures how much shape the neighborhood includes. The curvedness also provides scale information: a large negative value implies a very gentle change, whereas a large positive value implies a very sharp edge. In the 3D volumetric data, polyps generally appear as bulbous, cap-like structures adhering to the colonic wall, with small to medium curvedness, whereas folds appear as elongated, ridge-like structures with large curvedness. The colonic walls appear as nearly flat, cup-like structures with small curvedness. Therefore, the shape index and the curvedness can differentiate polyps from folds and colonic walls effectively.

Because of the partial volume effect, the soft-tissue density values within a polyp tend to smoothly increase from the colonic air toward the center of the polyp. Therefore, most density gradient vectors within a polyp tend to point toward the polyp center. A gradient concentration feature that characterizes the overall direction of the gradient vectors around a point is used for further reducing FPs.

The computation of these features for the entire volume is time consuming. In our pipeline, we compute these features in a way similar to the shape based CAD methods. However, the critical difference is

that we only compute these features on several suspicious areas for FP reduction, rather than for the entire colon.

4 Integration with Virtual Colonoscopy

The polyp detection results of our CAD pipeline are also stored with the flattened colon image, which can be used for highlighting the corresponding VC endoscopic view. The colon mesh extracted in our pipeline can also be used to accelerate the direct volume rendering of the VC endoscopic view.

4.1 Polygonal Assisted Volume Rendering

When navigating or flying through the colon lumen, the colon wall is rendered with direct volume rendering. Because of the large size of the colon volume data and the inherent complexity of volume rendering, it is very hard to achieve interactive frame rates with a software implementation. 3D texture-based volume rendering [5] is a popular volume rendering method that can achieve real-time speed on commodity graphics hardware (GPU). However, the rays shot from the image plane have different sampling rates due to the planar proxy geometry. Ray casting has been implemented on the GPU, which has a coherent sampling rate for all rays [13]. They have achieved interactive speed by using the two common acceleration techniques, empty-space skipping and early ray termination.

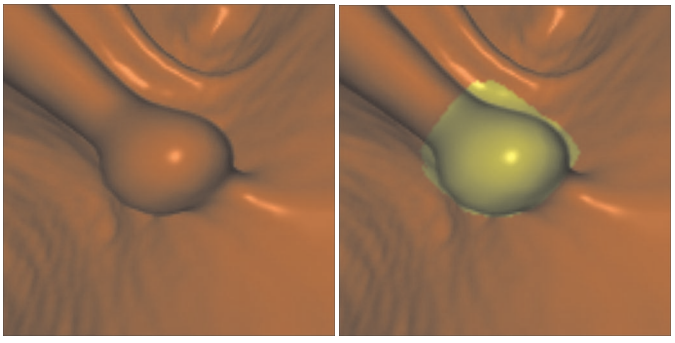

(a) (b)

Fig. 7. A close up view of a polyp rendered with volumetric ray casting (a) without coloring, and (b) with coloring.

The polygonal mesh has been exploited by us to accelerate direct volume rendering [2]. The polygonal mesh representing the object boundary is extracted from the volume in the second step of our pipeline. Each vertex is associated with its coordinates in volume texture space. The mesh is projected onto the image plane for calculating the entry points of rays, and the empty space between the image plane and the object boundary is skipped. Our detection result is also stored in a 2D image, in which we use yellow color for polyps and red color for normal colon wall. When the flattened mesh is projected on the image, we also obtain a 2D texture coordinates by interpolation. We use this 2D texture coordinates to access the resulting image to determine the color of the ray. This method is very efficient because the GPU is very efficient in rasterizing triangles onto the image plane.

Our algorithm has two passes. In the first pass, the mesh is rendered and the rasterization hardware interpolates the texture coordinates for each fragment. In this pass, the depth test is enabled so that only the nearest intersection points are preserved in the framebuffer. In the second pass, the fragment shader reads back the intersection point for each pixel on the image plane and a standard ray casting is performed from this point. A polyp rendered with our method with and without coloring is shown in Figure 7. The rendering frame rates is 17-20 per second for a 512×512 image.

4.2 User Interface

Our interactive user interface shown in Figure 8 provides multiple views of the colon CT data. The 2D mutually perpendicular slice views oriented axial, sagittal and coronal are shown on the right hand side. A flattened colon image is shown on the left hand side. In the center is the 3D volume rendered endoscopic view using the above polygon assisted algorithm. An outside overview of the patient's colon with bookmarks of suspicious patches and a zoom-in slice view are shown on the left of the endoscopic view. All these 2D and 3D images are correlated and interlinked so that position in 3D is overlaid on the 2D images and the position of 2D slices and the flattened colon image can be overlaid on the 3D images. This provides a quick and simple mechanism to easily analyze suspicious patches in both 2D and 3D.

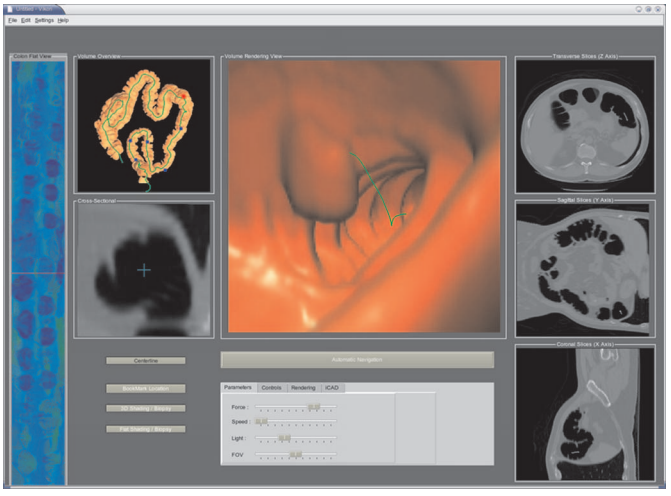

Fig. 8. The user interface of our CAD system.

We have integrated the detection result of our CAD pipeline into our VC system. Our new VC system is enhanced in the following ways:

1. In the navigation mode, the suspicious patches are highlighted in the endoscopic view to attract the attention of the radiologists during navigation. Since our detection algorithm is 100% sensitive to polyps, the missed polyps in the conventional VC system will not be missed in our system.

2. All suspicious polyp candidates are also highlighted on the 2D flattened colon view. Radiologists can directly inspect these suspicious regions by clicking on them. All other views are updated simultaneously.

3. Bookmarks for suspicious regions are stored on the flattened colon image and on the colon overview image. From either image, the radiologists can sequentially or randomly go through all bookmarks of suspicious regions, which are automatically provided by our CAD pipeline.

Our initial feedback from a radiologist using our prototype system has been very positive, where the CAD results serving as a second reader guarantee a low miss examination and that the user interface features indeed enhance the VC system.

5 Implementation and Results

We implemented our polyp detection pipeline in C/C++ and ran all of the experiments on a 3.6 GHz Pentium IV PC running Windows XP with 3G RAM and one NVIDIA Quadro 4500 graphics board. We have been collaborating closely with radiologists and gastroenterologists in developing and evaluating our methods. We used 52 CT data sets from the National Institute of Health (NIH) to demonstrate and test our CAD pipeline. Along with the raw DICOM images, there are VC reports, OC reports, pathology reports, and OC videos. In addition, we used another 46 CT data sets along with VC reports and OC reports obtained from Stony Brook University Hospital (SBUH) to test and demonstrate our pipeline. We used the specialists' VC and OC reports for the NIH and SBUH data sets to evaluate our CAD pipeline.

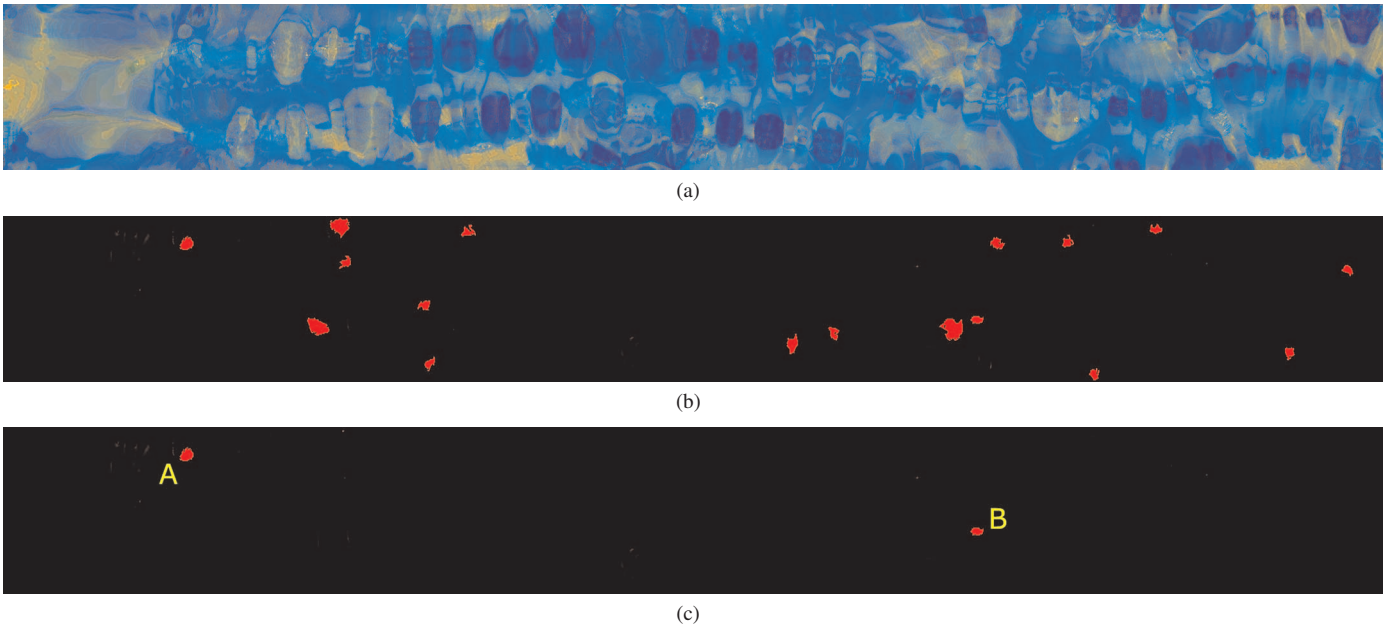

(a) (b) (c)

Fig. 9. (a) The electronic biopsy image generated using our conformal colon flattening and volumetric ray casting algorithm. (b) The result of our clustering algorithm. (c) The result of the reduction of FPs with shape analysis and 3D texture analysis.

Ten of the 52 NIH data sets were used to train our clustering algorithms, to compute the K-L matrix and the representative vector V. The rest of the data sets were used to test our CAD pipeline, which exhibits consistent results. The electronic biopsy images were all generated with the same biopsy transfer function. Our results show that our clustering algorithm is 100% sensitive to polyps, and no polyp from the 42 NIH data sets and the 46 SBUH data sets was missed. The polyps are colored using our volumetric ray casting algorithm with a translucent biopsy transfer function. All the polyps are shown in similar colors on the 2D image, which will not be missed by our clustering algorithm.

Table 1. Experimental results of our CAD pipeline.

Data Source	Total Polyps	FP per data set	FP Reduction
NIH	58	3.1	96.3%
SBUH	65	2.9	97.1%

The experimental results are shown in Table 1, which are confirmed using VC reports and OC reports. There are 58 polyps in the 42 NIH data sets. 96.3% FPs are eliminated in the reduction step. Our method has an average FP count of 3.1 per NIH data set after the FP reduction. There are 65 polyps in the 46 SBUH data sets. 97.1% FPs are eliminated in the reduction step. Our method has an average FP count of 2.9 per SBUH data set. The best shape analysis based systems [6, 19, 24, 28] achieved $2-3$ FPs per dataset with 100% sensitivity. Our experiment results show that our method achieved similar results as these systems.

One of the SBUH CT data sets of size $512 \times 512 \times 460$ has a polyp near the rectum. The resolution of the flattened electronic biopsy image is 4000×200, which is shown in Figure 9(a). The rectum is at the left end of Figure 9(a). There is a polyp of 8 mm diameter near the rectum of this colon data set. The suspicious polyp candidates from our clustering algorithm are shown in red in Figure 9(b). The FPs are reduced by shape analysis and 3D texture analysis applied at these suspicious areas. As a result, we obtain 2 polyp candidates, the real polyp at location A and a FP at location B, both shown in red in Figure 9(c). The corresponding 3D VC views of these two locations are shown in Figures 10(a) and 10(b), respectively. It is noted that the FP B is resulted from the protuberance on the colon haustral fold.

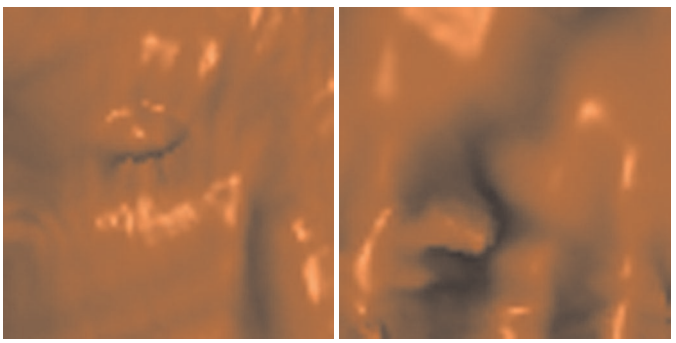

(a) (b)

Fig. 10. (a) The 3D view of the detected polyp A. (b) The 3D view of the false-positive finding B on a colon fold.

Compared with shape-based CAD methods, our system is much faster. Our topological denoising algorithm and colon surface extraction algorithm costs less than 1 minute. The most time consuming step of our pipeline is the conformal colon flattening, which takes about 7 minutes. The electronic biopsy image rendered with a resolution of 4000×200 costs only about 300 milliseconds accelerated on the GPU. Therefore, it takes our pipeline about 8 minutes to gather features for polyp detection. In the shape-based CAD methods, the computation step of shape index and curvedness is the most time consuming step. It took us about 20 minutes to compute shape index and curvedness with a mask size of $5 \times 5 \times 5$ for the entire mucosa layer, using the same data set on the same platform as our approach. The computation time is about one hour when the mask size is $7 \times 7 \times 7$. We achieved an average of 3 FPs per data set with 100% sensitivity, which is equal or better than the shape based methods. Our detection results are stored in 2D flattened images, which are much easier to integrate into the VC system than that of other CAD systems. Our pipeline provides a flattened colon view in the user interface of the VC system, which is much more friendly than the other systems.

6 Conclusions

We have presented a novel method for polyp detection using direct volume rendering. Our method is different from previous shape based methods, as we detect suspicious patches on a 2D volume rendered flattened biopsy image of the colon. This is due to the fact that the adenomatous and malignant polyps in the volume rendered biopsy images have different densities compared with normal tissues. The FPs are further reduced in a subsequent step by shape analysis and 3D texture analysis, which are only performed on the suspicious patches. Our system is 100% sensitive to polyps with a very low FP rate. The detection results are stored using 2D images, which are easily integrated into our VC system to highlight the polyp locations on the colon wall during navigation. We also provide a flattened colon view in our VC system. The missed areas and polyps in the conventional VC system are not missed in our enhanced VC CAD system. Thus, the radiologist can navigate within the colon model in just one direction. The radiologist who used our prototype CAD system reported examination time of about half the time of using a conventional VC system.

We are in the process of porting our CAD pipeline to a clinical VC system and plan to continue working closely with our collaborating domain experts to further evaluate the new technique in real world clinical settings. Since two scans (supine and prone) are taken for each patient, we would like to study the registration of supine and prone based on our conformal colon flattening technique. The registration results can be used to double check for polyp detection. Since our colon flattening algorithm is angle preserving, we would like to apply 2D shape fitting methods to detect polyps on the 2D electronic biopsy images. We also plan to try more advanced pattern recognition algorithms to further reduce our FPs.

Acknowledgements

This work has been partially supported by NSF grant CCR-0306438 and NIH grants CA082402 and CA110186. We disclose that one of the authors owns a fraction of Viatronix Inc. shares. The CT colon datasets are courtesy of the National Institute of Health and Stony Brook University Hospital. We are grateful to the laboratory for imaging research and informatics (IRIS) at Stony Brook and its director Zhengrong Liang for the use of their partial volume segmentation code [25]. We thank Joseph Marino for his help with the research work and proofreading.

References

[1] B. Acar, C. Beaulieu, S. Gokturk, C. Tomasi, D. Paik, R. B. Jeffrey, J. Yee, and S. Napel. Edge displacement field-based classification for improved detection of polyps in CT colonography. *IEEE Transactions on Medical Imaging*, 21:1461–1467, 2002.

[2] R. S. Avila, L. M. Sobierajski, and A. E. Kaufman. Towards a comprehensive volume visualization system. *IEEE Visualization*, pages 13–20, 1992.

[3] A. V. Bartroli, R. Wegenkittl, A. Konig, and E. Groller. Nonlinear virtual colon unfolding. *IEEE Visualization*, pages 411–418, Oct. 2001.

[4] G. Bertrand. Simple points, topological numbers and geodesic neighborhoods in cubic grids. *Pattern Recognition Letters*, 15:1003–1011, 1994.

[5] B. Cabral, N. Cam, and J. Foran. Accelerated volume rendering and tomographic reconstruction using texture mapping hardware. *Symposium on Volume Visualization*, pages 91–98, 1994.

[6] S. B. Göktürk, C. Tomasi, B. Acar, C. F. Beaulieu, D. S. Paik, R. B. Jeffrey, J. Yee, and S. Napel. A statistical 3D pattern processing method for computer aided detection of polyps in CT colonography. *IEEE Transactions on Medical Imaging*, 20(12):1251–1260, 2001.

[7] S. Haker, S. Angenent, A. Tannenbaum, and R. Kikinis. Nondistorting flattening maps and the 3D visualization of colon CT images. *IEEE Transactions on Medical Imaging*, 19:665–670, Dec. 2000.

[8] X. Han, C. Xu, and J. L. Prince. A topology preserving level set method for geometric deformable models. *IEEE Transactions on PAMI*, 25(6):755–768, 2003.

[9] L. Hong, S. Muraki, A. Kaufman, D. Bartz, and T. He. Virtual voyage: interactive navigation in the human colon. *SIGGRAPH*, pages 27–34, 1997.

[10] W. Hong, X. Gu, F. Qiu, M. Jin, and A. Kaufman. Conformal virtual colon flattening. *ACM Symposium on Solid and Physical Modeling*, pages 85–94, 2006.

[11] C. D. Johnson and A. H. Dachman. CT colonography: The next colon screening examination? *Radiology*, 216(2):331–341, 2000.

[12] G. Kiss, J. Cleynenbreugel, M. Thomeer, P. Suetens, and G. Marchal. Computer-aided diagnosis in virtual colonography via combination of surface normal and sphere fitting methods. *European Journal of Radiology*, 12:77–81, 2002.

[13] J. Kruger and R. Westermann. Acceleration techniques for GPU-based volume rendering. *IEEE Visualization*, pages 38–44, 2003.

[14] J. S. Mandel, J. H. Bond, T. R. Church, D. C. Snover, G. M. Bradley, L. M. Schuman, and F. Ederer. Reducing mortality from colorectal cancer by screening for fecal occult blood. *New England Journal of Medicine*, 328(19):1365–1371, 1993.

[15] J. Nappi, H. Frimmel, A. Dachman, and H. Yoshida. Computerized detection of colorectal masses in ct colonography based on fuzzy merging and wall-thickening analysis. *Medical Physics*, 31:860–872, 2004.

[16] J. Nappi and H. Yoshida. Feature-guided analysis for reduction of false positives in cad of polyps for CT colonography. *Medical Physics*, 30:1592–1601, 2003.

[17] D. S. Paik, C. F. Beaulieu, G. D. Rubin, B. Acar, R. B. Jeffery, J. Yee, J. Dey, and S. Napel. Surface normal overlap: a computer-aided detection algorithm with application to colonic polyps and lung nodules in helical CT. *IEEE Transactions on Medical Imaging*, 23(6):661–675, June 2004.

[18] P. J. Pickhardt, J. R. Choi, I. Hwang, J. A. Butler, M. L. Puckett, H. A. Hildebrandt, R. K. Wong, P. A. Nugent, P. A. Mysliwiec, and W. R. Schindler. Computed tomographic virtual colonoscopy to screen for colorectal neoplasia in asymptomatic adults. *The New England Journal of Medicine*, 349(23):2191–2200, Dec. 2003.

[19] R. M. Summers, C. D. Johnson, L. M. Pusanik, J. D. Malley, A. M. Youssef, and J. E. Reed. Automated polyp detection at CT colonography: Feasibility assessment in a human population. *Radiology*, 219(1):51–59, 2001.

[20] C. Tomasi and S. B. Göktürk. A graph method for the conservative detection of polyps in the colon. *2nd International Symposium on Virtual Colonoscopy*, 2000.

[21] D. Vining, Y. Ge, D. Ahn, and D. Stelts. Virtual colonoscopy with computer-assisted polyps detection. *Computer-Aided Diagnosis in Medical Imaging*, pages 445–452, 1999.

[22] M. Wan, F. Dachille, K. Kreeger, S. Lakare, M. Sato, A. Kaufman, M. Wax, and J. Liang. Interactive electronic biopsy for 3D virtual colonoscopy. *SPIE Medical Imaging*, 4321:483–488, 2001.

[23] G. Wang and M. W. Vannier. GI tract unraveling by spiral CT. *Proceedings SPIE*, 2434:307–315, 1995.

[24] Z. Wang, Z. Liang, L. Li, X. Li, B. Li, J. Anderson, and D. Harrington. Reduction of false positives by internal features for polyp detection in CT-based virtual colonoscopy. *Medical Physics*, 32(12):3602–3616, 2005.

[25] Z. Wang, Z. Liang, X. Li, L. Li, D. Eremina, and H. Lu. An improved electronic colon cleansing method for detection of colonic polyps by virtual colonoscopy. *IEEE Transactions on Biomedical Engineering*, 53:1635–1646, 2006.

[26] J. Yao, M. Miller, M. Franaszek, and R. Summers. Colonic polyp segmentation in CT colonoscopy-based on fuzzy clustering and deformable models. *IEEE Transactions on Medical Imaging*, 23:1344–1352, 2004.

[27] H. Yoshida, Y. Masutani, P. MacEneaney, D. T. Rubin, and A. H. Dachman. Computerized detection of colonic polyps in CT colonography based on volumetric features: A pilot study. *Radiology*, pages 327–336, Jan. 2002.

[28] H. Yoshida and J. Näppi. Three-dimensional computer-aided diagnosis scheme for detection of colonic polyps. *IEEE Transactions on Medical Imaging*, 20(12):1261–1274, 2001.

[29] N. Zhang, W. Hong, and A. Kaufman. Dual contouring with topolgy-preserving simplification using enhanced cell representation. *IEEE Visualization*, pages 505–512, Oct. 2004.